

## Demonstration of degaussing by copper and HTS windings

D Wikkerink<sup>a\*</sup>, I Hanse<sup>b</sup>, A Rodrigo Mor<sup>a</sup>, H Polinder<sup>a</sup>, R Ross<sup>a</sup>

<sup>a</sup>Delft University of Technology, The Netherlands; <sup>b</sup>University of Twente, The Netherlands

\*Corresponding author. Email: d.p.wikkerink@tudelft.nl

### Synopsis

Due to their permeability, merchant and naval vessels distort Earth's magnetic field which leaves a magnetic signature. These anomalies in the magnetic field may be detected by mines leaving the vessel exposed. To avoid detection by magnetic sensors, the vessels magnetic signature can be reduced in several ways. One of them is degaussing: a technique where a set of on-board coils produces a magnetic field to cancel the magnetic signature. Modelling studies have shown that the performance of a degaussing system can be improved by replacing the copper with high temperature superconductor (HTS) coils in terms of volume, weight and energy efficiency. This study aims to compare the degaussing functionality of copper and HTS windings. A table-top demonstration model is presented which is equipped with both copper and HTS degaussing coils. The demonstrator is prepared by removing the permanent magnetisation. The two degaussing topologies are compared in terms of functionality, efficiency, controllability and mutual inductances.

Keywords: Degaussing; HTS; Superconductor; Magnetic signature; Deperming

### 1. Introduction

Some naval mines are able to detect the proximity of a ship by measuring an anomaly in Earth's magnetic field. The ship alters the local magnetic field. The profile of the magnetic flux density around the ship, or magnetic signature, is characterized by the geometry and the material of the ship. There are several components which make up the magnetic signature. The most important ones are listed below.

*Induced magnetisation* is the portion of the magnetic signature which is induced directly by the magnetic field of the Earth. The steel structure of a ship has a much higher permeability than the air and water around it, so the hull provides a path of least magnetic reluctance. The magnetic flux of Earth's magnetic field is drawn to it and accumulates in the hull. Consequently, the magnetic flux density around the ship is affected by this. The induced magnetisation can be removed by degaussing.

*Permanent magnetisation* occurs because ferromagnetic materials, like a standard steel used for the hull of a ship, have the property to leave a residual flux after an external field is removed or changed. During sailing, the ship gets magnetised over time. For this reason, the permanent magnetisation must be measured and removed periodically. Also, a permanent field can build up when the ship is oriented in the same direction for a long period of time. For example, during the construction or when it is docked. Permanent magnetisation can be removed by deperming and degaussing.

*Eddy currents* are induced in the hull when the ship is moving through a magnetic field. In turn, these currents produce their own magnetic field that contributes to the magnetic signature. Eddy currents are produced by all ship motions in Earth's magnetic field. However, since the intensity of eddy currents is proportional to the rate of change of position within the magnetic field, eddy currents due to the pitching motion are the most prominent. Because eddy currents are induced in any conductor, it doesn't matter whether the hull is made of ferromagnetic material or not.

*Corrosion currents* occur because the salty sea water closes the electrical circuit between the potential difference of different materials, like the ship's hull and the propeller. Again, the currents produce a magnetic field which contributes to the magnetic signature. Eddy and corrosion currents can be counteracted with degaussing.

*On-board equipment* like electrical machines, power converters, switch gear and power cables produces magnetic noise. Most of this noise, especially at high frequencies, is shielded by the hull.

Detection of the ship can be avoided by reducing the magnetic signature. An obvious, passive way would be to replace the steel hull by a non-ferromagnetic material like fiberglass, titanium or some types of stainless steel, but this is not always practical. These materials can be expensive, difficult to handle or don't provide enough structural strength. Another, active way to reduce the magnetic signature is by degaussing. A degaussing system is a set of on-board coils which generate a magnetic field that counter-acts the induced magnetisation. Ideally, the magnetic field created by the degaussing coils exactly opposes the induced field, so that the magnetic signature is cancelled. Degaussing coils are placed in the longitudinal (L-coils), athwart ship (A-coils) and in the vertical (M-coils) direction of the ship.

Today, degaussing coils are made of copper. Although copper is a very good conductor, a copper degaussing coil still produces a significant amount of heat by Ohmic losses. Additionally, copper degaussing systems are heavy and large. An alternative would be to use high temperature superconductor (HTS) coils. It is expected that HTS degaussing coils can improve the energy efficiency of a degaussing system significantly (Ross, 2012). The resistance in a superconductor is (nearly) zero, so the Ohmic losses in the coils are eliminated. Also, the current density in HTS can be much higher than in copper, which results in a more compact degaussing system. The main challenge is that HTS needs to be cooled down to cryogenic temperatures to become superconductive. Another challenge will be the controllability of a HTS degaussing coil. Because of the large inductance, but zero resistance, HTS degaussing coils will have a large time constant. A pilot study has already been done by replacing one of the copper degaussing coils with an HTS coil on the naval vessel USS Higgins using a helium gas cooled cryostat (Kephart, 2011).

The goal of the present paper is to compare the functionalities of an HTS degaussing system with a copper degaussing system. This is done with a table-top demonstrator which is equipped with both copper and HTS degaussing coils. The two degaussing topologies are compared by measuring the corresponding reduced magnetic signatures. A preliminary study was done where the magnetic signature reduction with only copper coils was measured (Wikkerink, 2019).

## 2. Benefits and issues using HTS

The use of HTS degaussing coils eliminates any Ohmic losses in the coils. However, two extra sources of power loss are introduced. Firstly, HTS can only function when it is cooled down to a temperature where it is in a superconductive state. This causes cooling losses. Secondly, HTS can handle a high current density, so it might be useful to design the degaussing coils with fewer turns and higher current than with the copper degaussing coil. This will save material, but will also cause an increase in the energy dissipation in the source because of the higher current. From an efficiency point of view, HTS is only beneficial when these two loss sources are smaller than the initial Ohmic losses from a copper degaussing system. This is a trade-off which depends on the size of the system.

With the lack of a resistance in the HTS degaussing coils, the time constant might become too big to control the current through the coil. The equation below shows how the time constant  $\tau$  of a coil depends on its inductance  $L$  and series resistance  $R$ .

$$\tau = \frac{L}{R}$$

With  $R$  going to zero, the time constant becomes very large. This is problematic when the system needs to react fast. In a practical case however, the power source has an internal series resistance. Also the leads from the power source to the superconductor are made of copper, so there will be a source of damping in the system. Moreover, if fewer number of turns are used in the HTS system, the inductance of the degaussing coils, and therefore the time constant, will decrease as well.

For a system of degaussing coils, the coupling of the coils might play a role because of the lack of damping. The following equation describes the coupling of a degaussing coil with the rest of the coils in a system of degaussing coils.

$$u_1 = R_1 i_1 + L_1 \frac{d}{dt} i_1 + \sum_1^n M_{1n} \frac{d}{dt} i_n$$

In an HTS system, the term with the series resistance might become so small that the mutual inductance,  $M$ , becomes significant. This means that the degaussing coil is more responsive to the current running through the coupled coils. Again, the series resistance does not go to zero because of the power source and the current leads.

## 3. System description

### 3.1. Design of the test setup

The table top demonstrator consists of a hollow steel pipe with caps welded on the ends to simulate a ship. The pipe is equipped with degaussing coils in two directions, one in the  $M$ , i.e., vertical direction and two in the  $L$ , i.e., longitudinal direction. For each degaussing coil there is a copper and HTS variant which are placed as close to each other as possible, so almost in the same position. The demonstrator is placed parallel to the magnetic meridian, so the magnetic distortion is expected to take place in two dimensions. The degaussing can then also be done in

two dimensions which makes a coil in the athwart ship direction unnecessary. A schematic representation of the demonstrator is depicted in Figure 1.

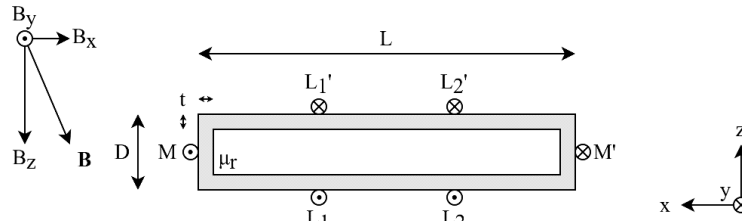


Figure 1: Schematic representation of the test setup

Where  $L$  is the length of the pipe,  $D$  is the diameter of the pipe,  $t$  is the thickness of the pipe and  $\mu_r$  the relative permeability of the pipe.  $B_x$ ,  $B_y$  and  $B_z$  are the Cartesian components of the magnetic flux density of Earth's magnetic field with respect to reference frame  $x$ ,  $y$  and  $z$ .  $M$ ,  $L_1$ , and  $L_2$  represent the three degaussing coil positions for which each position has a copper and HTS degaussing coil. The values of the parameters are listed in Table 1.

Table 1: Parameters of the demonstrator

Name	Description	Value	Unit
$L$	pipe length	1500	mm
$D$	pipe diameter	320	mm
$t$	wall thickness	5	mm
$\mu_r$	relative permeability	320	-
$B_x$	flux density in x direction	18.02	$\mu\text{T}$
$B_y$	flux density in y direction	0.07	$\mu\text{T}$
$B_z$	flux density in z direction	42.45	$\mu\text{T}$

The values of  $B_x$ ,  $B_y$  and  $B_z$  are the average of the measured magnetic flux density over the distance of the measuring line without the pipe in place, this is further explained in section 2.3. Since the pipe is placed parallel to the magnetic north south line, the  $y$  component of the measured zero field is close to zero. The relative permeability is found by fitting the measurement of the magnetic signature to the simulated magnetic signature.

### 3.2. Definition of the tests

Two tests were conducted in order to find out whether HTS and copper degaussing are similar. The static test is a set of measurements where the demonstrator is in a fixed position in the magnetic field of the Earth. First, the magnetic signature of the pipe is mapped by moving a magnetic sensor underneath the demonstrator over a 4 meter distance. Then the reduced magnetic signature is measured with the copper degaussing coils on and then the reduced magnetic signature is measured with the HTS degaussing coils on.

The dynamic test involves a pitching motion of the demonstrator. When the pipe is pitched within Earth's magnetic field, the magnetic signature will change. During the test, the pitching angle of the pipe is measured. The degaussing current set points are set accordingly with a control loop. First, the magnetic signature is measured on the five points as a function of pitching angle. Then the reduced magnetic signature by means of copper degaussing is measured and finally the reduced magnetic signature by means of HTS degaussing is measured. Figure 2 shows a schematic representation of the two tests.

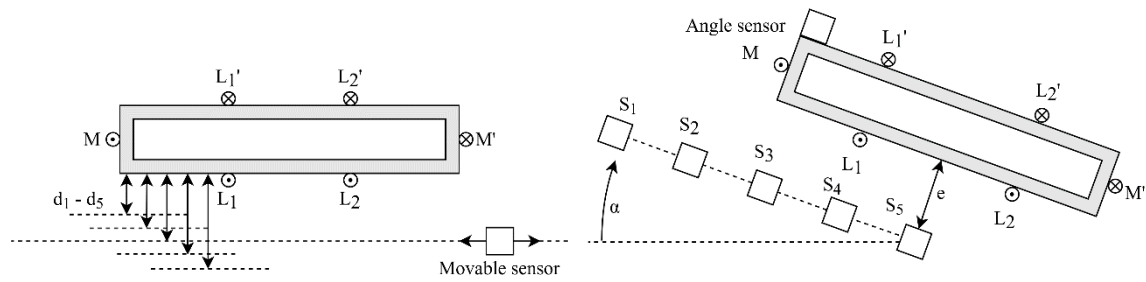


Figure 2: Schematic representation of static (left) and dynamic (right) test

Where  $d_1$  to  $d_5$  are the measuring distances from the outside of the pipe to the movable sensor,  $e$  is the measuring distance from sensors  $S_1$  to  $S_5$  to the outside of the pipe and  $\alpha$  is the pitching angle of the pipe. The parameters of the two tests are listed in Table 2.

Table 2: Sensor parameters

Name	Description	Value	Unit
$e$	Measuring distance in the dynamic test	445	mm
$d_1, d_2, d_3, d_4, d_5$	Measuring distances of the sensor to the pipe wall in the static test	439, 389, 339, 289, 239	mm
$S_1, S_2, S_3, S_4, S_5$	Sensor 1, 2, 3, 4 and 5 with distance from the centre of the pipe.	0, 300, 600, 900, 1200	mm
$\alpha$	Pitching angle range	0 – 25	degrees

### 3.3. Background field

The test setup was built in a wooden building where Earth’s magnetic field was expected to be uniform and stronger than within a steel construction. Before the test were done, the magnetic field in the room needed to be mapped. Figure 3 shows the flux density of the three components of Earth’s magnetic field over a distance of 4 meters where the magnetic sensor is able to move.

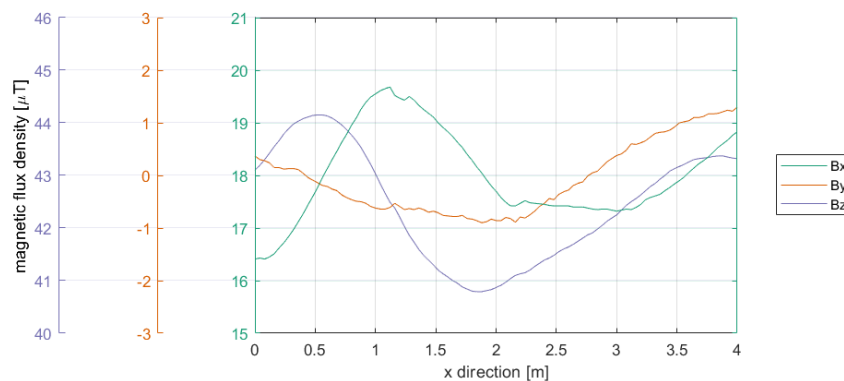


Figure 3: Components of the background field

Although the background magnetic flux density was expected to be homogeneous, the measurements show a deviation of almost 4  $\mu\text{T}$  in the  $x$  and  $z$  component of the measured field. This is probably due to the magnetic signature of the construction of the building where the test setup was placed. The values for  $B_x$ ,  $B_y$  and  $B_z$  in Table 1 are the averages of the data in Figure 3. The magnitude of Earth’s magnetic field is mapped at several measuring heights. The results are shown in Figure 4.

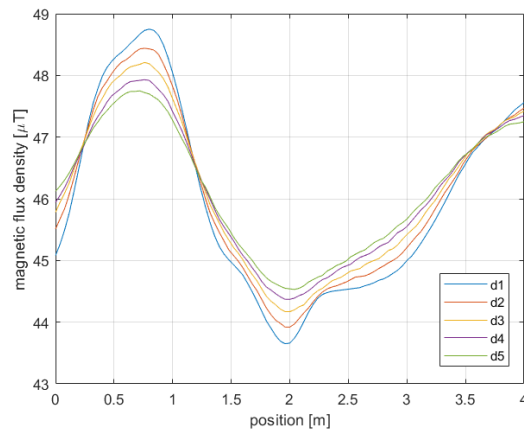


Figure 4: Measurement of the background field at different heights

It can be observed that Earth's magnetic field gets more uniform as the sensor moves away from the floor. An explanation for this could be a steel reinforced floor which interferes with the measurements. The measurements from Figure 4 are used as a reference measurement for the following measurements. The measurements of the background field will be subtracted from the magnetic signature measurements, so that only the magnetic signature remains. By doing this, also an unwanted offset in the magnetic sensors is removed.

## 4. Realisation

### 4.1. Simulations

There are several ways to model the magnetic field around a steel object. An analytical approach may be used when the geometry of the object resembles a spherical or ellipsoidal geometry (Baker, 1982). In this method, Maxwell's equations are solved in a spheroidal or ellipsoidal coordinate system. The cylinder in this test setup can be approximated by a hollow ellipsoid. The results of the analytical approach for this test setup are shown in Figure 7. An analytical model is useful for fast calculations in feedback loops, fast approximations or optimisation loops. When the geometry gets more complicated and more accurate results are needed, finite element modelling (FEM) gives a better result (Aird, 2000). The simulated magnetic signature and the reduced magnetic signature are shown in Figure 5.

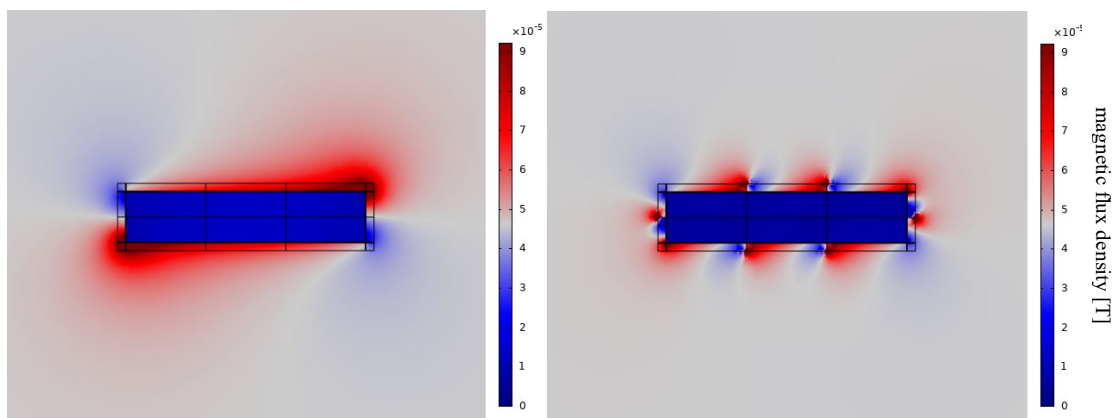


Figure 5: Simulation of the magnetic signature (left) and the reduced magnetic signature (right)

The colour map on the left side of Figure 5 shows the magnetic signature of the pipe when it is placed in Earth's magnetic field. The values for the external field are taken from Table 1. The figure on the right shows the colour map of the pipe when there is a current in the degaussing coils. It is clear that the degaussing system reduces the magnetic signature of the pipe. The coupling factors between the M, L1 and L2 coils are simulated using the same FEM model. The results are shown in Table 3. The coupling factors are also computed for the case that the degaussing coils are mounted on the inside of the pipe. These are shown in Table 4.

Table 3: coupling factors (external coils)

	M	L1	L2
M	1	0.102	0.102
L1	0.102	1	0.150
L2	0.102	0.150	1

Table 4: coupling factors (internal coils)

	M	L1	L2
M	1	0.00001	0.0001
L1	0.0001	1	0.004
L2	0.0001	0.004	1

From these tables it can be seen that the degaussing coils in the demonstrator might be responsive to the current in other degaussing coils because of the high coupling factors. However, in the case where the coils are mounted on the inside of the pipe, the coupling of the coils is very low. The flux paths are not enclosed by the other coils, because most of the flux is going through the hull. This will be closer to the reality because, on a ship, the degaussing coils will also be mounted on the inside.

#### 4.2. Magnetic signature

A photo of the test setup is shown in Figure 6. On the left the metal pipe is shown with end caps welded on the sides. The material of the pipe is S355J2H, a high tensile steel which is used for the construction of ships. The HTS degaussing coils are placed inside cryostats for insulation and cooling. The copper degaussing coils are simple insulated copper wires which are wound around the pipe. The measurement rail is placed underneath the pipe. The pipe is placed in a wooden construction which makes it possible to place it under different angles with respect to Earth's magnetic field. This is used in the dynamic test to simulate a pitching motion. The angle is measured with an acceleration sensor. The acceleration is integrated twice to obtain the angle. The angle sensor and the five magnetic sensors are fixed to the wooden construction. The cryostats of the HTS degaussing coils are connected to a closed liquid nitrogen system to ensure that the coils maintain their superconductive state. The sensor cart for the static measurements is shown in the right photo of Figure 6. The height of the sensor is changed by adjusting the nuts on the non-magnetisable threads.

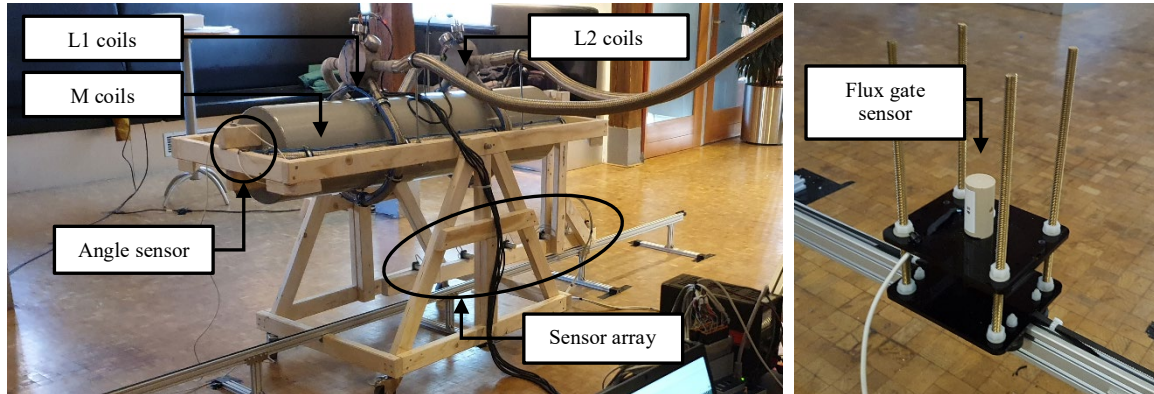


Figure 6: Photo of the demonstrator (left) and the sensor cart (right)

The magnetic flux density is measured by flux gate sensors. These sensors are very sensitive, but have a relatively low accuracy. Therefore, all the measurements are normalized with a reference measurement. This eliminates any offset in the sensors. In order to avoid any disturbances in the measurements, all the materials in the test setup are chosen to have a relative permeability of close to one. The magnetic signature of the pipe is determined by subtracting the measurement of the pipe first measuring the magnetic field without the pipe.

The measured magnetic signatures are shown in Figure 7. The left graph shows a comparison with the different modelling approaches. It can be seen that the results of the FEM model are very similar to the measurements. The ellipsoidal analytical model (described in section 3.1) does not match the measurements that well. The horizontal position of the peaks of the magnetic signature is different than the measurements. This is because the analytical model uses an ellipsoidal geometry to approximate the cylindrical shape of the demonstrator. Still, it can be used for an estimation of the order of magnitude of the magnetic signature. The exact horizontal position of the peaks in the context of this experiment is not relevant, because the position of the peaks also depends on the location of the vessel. Ultimately, it's the variation in the magnetic field which triggers the sensor in a magnetic mine.

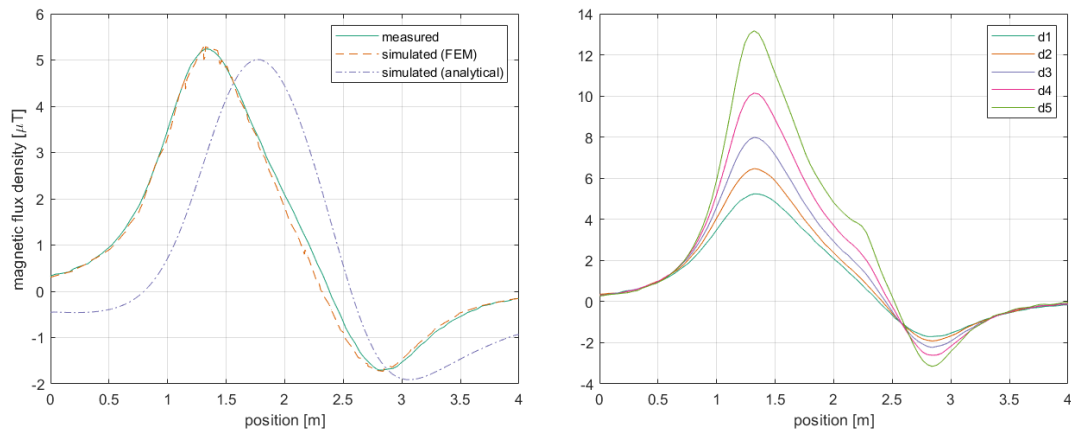


Figure 7: Magnetic signature measured versus simulated (left) and at several measuring distances (right)

The right plot in Figure 7 shows the measured magnetic signature with the sensor positioned at several measuring heights. The values for these measuring heights are given in Table 2.

#### 4.3. Deperming

To ensure that the measured magnetic signature corresponds to the simulated magnetic signature, any permanent magnetisation has to be removed from the pipe. Due to the magnetic hysteresis of the pipe, a residual magnetic flux remains when the pipe gets magnetised. This remanent flux can be removed by cyclic magnetising and demagnetising of the pipe. Every cycle, some residual flux will remain. However, if the amplitude of the magnetising field is reduced every cycle, the residual flux will reduce and eventually disappear. (Baynes, 2002). The pipe is magnetised and demagnetised by a deperming coil. Figure 8 shows a photo of the pipe with the deperming coil.

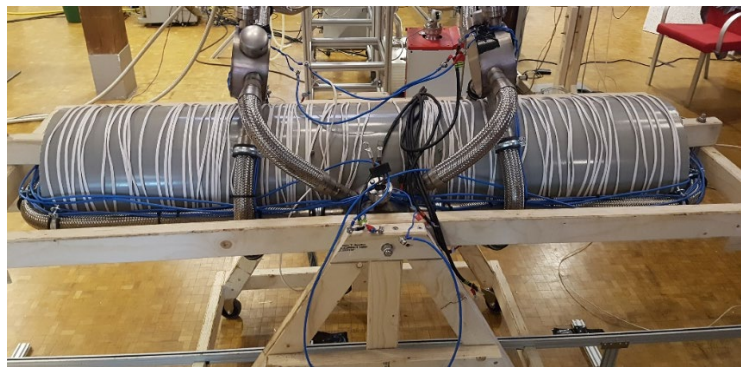


Figure 8: Deperming coil in the longitudinal direction

In this case, the magnetising current has a frequency of 2 Hertz and an amplitude of 1540 Ampere turns at the start of the deperming session. The amplitude was decreased to zero over a period of 180 seconds. It is important to ensure that the deperming process is done while the background field is zero (Holmes, 2008). A DC current was maintained in both the L deperming coil and the M degaussing coils so the horizontal and vertical components of Earth's magnetic field were compensated for. The graph in Figure 9 shows the results of the deperming process.

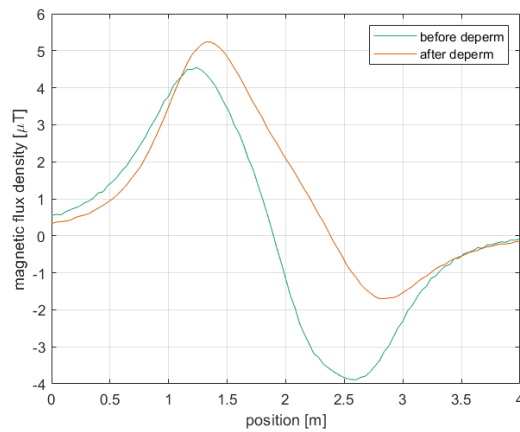


Figure 9: Magnetic signature before and after deperming

The magnetic signature changed significantly due to the deperming. The magnetic signature after the deperming shows a good resemblance with the simulated magnetic signature (Figure 7). This implies that the deperming process was successful.

## 5. Results

### 5.1. *Separate coils*

The difference between the behaviour of HTS and copper degaussing coils is investigated by measuring the effect of each coil independently. The effect of one degaussing coil can be measured by running a current through this coil and measuring the magnetic signature of the whole setup. Then, the magnetic signature of the setup with zero current through the coil is subtracted. Now only the effect of the coil remains. A measurement was done where each coil was powered with 15 ampere turns. Figure 10 shows the results.

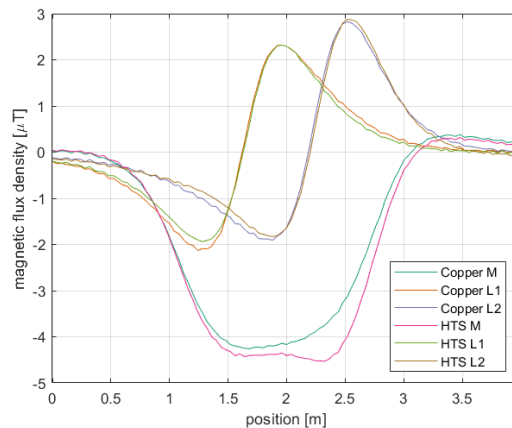


Figure 10: Effect of each degaussing coil

The HTS degaussing coils show very similar behaviour to the copper degaussing coils. There are some small differences visible. This is most likely because the copper and HTS degaussing coils could not be placed on the exact same location.

### 5.2. *Static test*

In the static test, the magnetic signature of the demonstrator is measured while the demonstrator is in a fixed position in Earth's magnetic field. First a reference measurement was done without the pipe in place. This measurement is subtracted from the following measurements to get the inhomogeneity of the background field out of the results. Then the magnetic signature is measured with the pipe in place following by the reduced magnetic signatures of both the copper as the HTS degaussing coils. Figure 11 shows the results of these measurements.



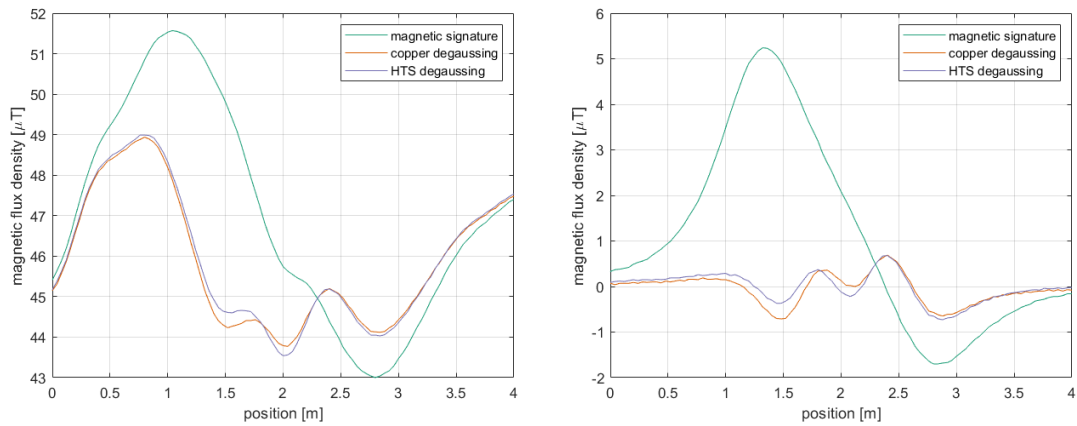


Figure 11: Static test results

The graph on the left side shows the absolute values of the measurements, where the reference measurement is not subtracted from the final measurements in this graph. The graph on the right side shows the normalized results. It can be seen that the copper and HTS degaussing coils behave very similar. A small difference is observed between both cases which most likely has to do with the placement of the coils.

### 5.3. Dynamic test

In the second test, the dynamic behaviour of the setup was tested. The pipe was pitched at an angle ranging from zero to twenty-five degrees. As with the static test, the background field was measured without the pipe in the vicinity. This measurement was later on subtracted from the magnetic signature measurements. Then the pipe was introduced and pitched over twenty-five degrees. After measuring the magnetic signature, the actual dynamic degaussing performance was measured. First the copper coils were tested where the current set-points were adjusted according to the pitching angle. Finally, the HTS degaussing performance was tested. The results are shown in Figure 12.

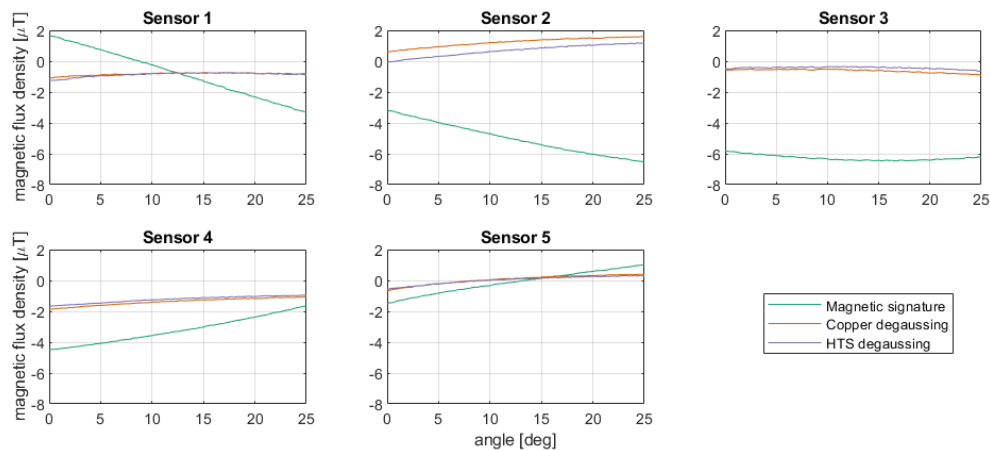


Figure 12: Dynamic test results

Overall, the copper and HTS coils have a very similar performance. A small difference between copper and HTS degaussing can still be seen, especially for sensor  $S_2$ . The difference which is observed is attributed to the difference in placement of the coils which has been discussed in section 4.1.

## 6. Conclusion

The main goal of the demonstrator tests was to demonstrate the equivalent behaviour of HTS degaussing coils compared to copper degaussing coils, and that HTS coils can thus be qualified as degaussing coils on ships. The magnetic behaviour of both copper and HTS degaussing coils is presented in this paper. Overall, both in the static and the dynamic experiments, the copper and HTS coils show a similar behaviour. The difference in magnetic

field between the both sets of coils is small and can be explained by small differences in the positions of the coils. The degaussing performance of both sets of coils is the same.

The differences between the HTS and copper L1 and L2 coils is smaller than the difference between the M coils. It is unclear where this difference comes from, but this might also have to do with the position of these coils. Also the construction around the pipe might have an influence on the magnetic signature. More simulation work and experiments are needed to answer this question.

The static test is a good way to visualize and compare the differences between copper and HTS degaussing. These tests gave an insight in the possibilities of using HTS for a degaussing system. The dynamic test is used to test the control system and the dynamics of the degaussing currents. In this test setup, the effect on the dynamics is not notable because the resistance of the degaussing coils is only a small portion of the total resistance in the system. The cables connecting the power supplies to the degaussing coils and the power supplies themselves are also resistive. There was not a notable difference between the time constant of the copper and HTS coils. To further investigate the dynamic effects of HTS coils in a degaussing system, a larger setup is needed so the large time constant of the superconductive coil without damping becomes more present, which would be the case in a full sized ship. In such a setup, the energy efficiencies of both systems will be comparable as well. The power consumption of an optimized cryostat would be relatively low so a fair comparison can be made with the Ohmic losses in a copper degaussing system. The coupling factors of the degaussing coils in a ship are so small that they are negligible.

For the experiments conducted, the permeability of the pipe was determined by fitting the measurements of the magnetic signature to simulated magnetic signature. In the future, the permeability of the pipe could be measured directly with an independent measurement. The deperming of the pipe only took place in the longitudinal direction. The magnetising field from the deperming coil might not have affected the end caps of the pipe. A deperming coil in the vertical direction could be employed for this.

### Acknowledgements

This project was enabled by RH Marine, IWO and DMO.

### References

- Aid GJC. 2000. Modelling the induced magnetic signature of naval vessels [dissertation]. Glasgow: University of Glasgow
- Baker FE, Brown SH. 1982. Magnetic induction of ferromagnetic prolate spheroidal bodies and infinitesimally thin current bands. *Journal of Appl. Physics*. 53:3991-3996.
- Baynes TM, Russel GJ, Bailey A. 2002. Comparison of stepwise demagnetization techniques, *IEEE Trans. Mag.*, 38(4).
- Holmes JJ. 2006. Exploitation of a ship's magnetic field signatures. [Place unknown]. Morgan & Claypool.
- Holmes JJ. 2008. Reduction of a ship's magnetic field. [Place unknown]. Morgan & Claypool.
- Kephart JT, Fitzpatrick BK, Ferrara P, Pyryt M, Pienkos J, Golda EM. 2011. High temperature superconducting degaussing from feasibility to fleet adoption. *IEEE trans. appl. supercond.* 21:2229-2232
- Ross R, Meijer CG, van de Mheen RJ. 2012. Degaussing by normal and superconductive windings. Proc. 11<sup>th</sup> INEC. May 15-17. Edinburgh.
- Wikkerink D, Rodrigo Mor A, Polinder H, Ross R. 2019. Design of a test setup to measure magnetic signature reduction. Proc. ICMET. Nov 5-7. Muscat